JGP Journal of General Physiology

RESEARCH ARTICLE

Determinants of selective ion permeation in the epithelial Na^+ channel

Lei Yang and Lawrence G. Palmer

The epithelial Na^+ channel (ENaC) is a key transporter mediating and controlling Na^+ reabsorption in many tight epithelia. A very high selectivity for Na^+ over other cations, including K^+, is a hallmark of this channel. This selectivity greatly exceeds that of the closely related acid-sensing channels (ASICs). Here, we assess the roles of two regions of the ENaC transmembrane pore in the determination of cation selectivity. Mutations of conserved amino acids with acidic side chains near the cytoplasmic end of the pore diminish macroscopic currents but do not decrease the selectivity of the channel for Na^+ versus K^+. In the WT channel, voltage-dependent block of Na^+ currents by K^+ or guanidinium$^+$, neither of which have detectable conductance, suggests that these ions permeate only ∼20% of the transmembrane electric field. According to markers of the electric field determined by Zn^{2+} block of cysteine residues, the site of K^+ block appears to be nearer to the extracellular end of the pore, close to a putative selectivity filter identified using site-directed mutations. To test whether differences in this part of the channel account for selectivity differences between ENaC and ASIC, we substitute amino acids in the three ENaC subunits with those present in the ASIC homotrimer. In this construct, Li:Na selectivity is altered from that of WT ENaC, but the high Na:K selectivity is maintained. We conclude that a different part of the pore may constitute the selectivity filter in the highly selective ENaC than in the less-selective ASIC channel.

Introduction

The epithelial Na channel (ENaC) is a component of the system that transports Na^+ into the circulation from transcellular compartments such as the urine and feces, or from fluids outside the body in the case of amphibian skin (Garty and Palmer, 1997; Kellenberger and Schild, 2002). It mediates the uptake of Na^+ into the cell across the apical plasma membrane, driven by an electrochemical activity gradient, after which the ion is removed from the cell across the basal and lateral membranes by active transport. An extremely high selectivity for Na^+ over K^+ is a hallmark of ENaC function; in most cases, the Na:K permeability or conductance ratios are stated as lower limits. In one study in which K^+ transport through the channels of toad urinary bladder was measured, the permeability ratio was estimated to be at least 500:1 (Palmer, 1987). This high selectivity may be of physiological importance, as the channel operates continuously, and even a small permeability to K^+ would result in substantial losses of this electrolyte over time.

The precise location of the selectivity filter in the channel protein is uncertain. Several studies performed shortly after the cloning of the three subunits of the channel (α, β, and γENaC; Canessa et al., 1994) identified amino acids presumed to be near the extracellular interface of its transmembrane pore as a likely site for the filter, as mutations at this site often reduced cation selectivity (Kellenberger et al., 1999a,b, 2001; Snyder et al., 1999; Sheng et al., 2000). These residues all have neutral side chains, analogous to the glycine–tyrosine–glycine signature selectivity sequence of K^+ channels. In contrast, a recent investigation of the closely related acid-sensing channel (ASIC) 1 identified a different region closer to the cytoplasmic interface that is essential for the selectivity of that pore (Lynagh et al., 2017). This part of the channel contains six conserved acidic amino acids—two on each subunit. When mutated to neutral species such as glutamine, or even when the length of the negatively charged side chain was altered, the selectivity for Na:K decreased substantially.

The selectivity of ASIC1 is much lower than that of ENaC (Yang and Palmer, 2014) so that it is possible that different mechanisms and different parts of the channel protein comprise the selectivity filter in the two channels. However, the acidic region of the ASIC1 pore is also conserved in ENaC, and its role in determining selectivity has not been systematically examined. Here we investigate the roles of the two candidate filter structures using several complementary approaches.

Department of Physiology and Biophysics, Weill-Cornell Medical College, New York, NY.

Correspondence to Lawrence G. Palmer: lgpalm@med.cornell.edu.

Materials and methods

Molecular constructs

Plasmids containing rat ENaC α, β, and γ subunits (Anantharam et al., 2006) were linearized with NotI restriction enzyme (New England Biolabs); complementary RNAs were transcribed with T7 RNA polymerase using the mMESSAGE mMACHINE kit (Ambion). Complementary RNA pellets were dissolved in nuclease-free water and stored in −70°C before use. Mutations were constructed using the Quick Change kit from Strategene following the manufacturer's instructions. Sequences were confirmed by GENEWIZ.

Two-electrode voltage clamp

Xenopus laevis oocytes (Ecocyte) were injected with 10 ng of RNA and incubated for 1–2 d in L-15 solution (Sigma-Aldrich) supplemented with HEPES (pH 7.4), penicillin 63 mg L^{-1}, and streptomycin 145 mg L^{-1} at 18°C. All chemicals were from Sigma-Aldrich unless otherwise noted.

For measurement of macroscopic currents, oocytes were placed in a rapid-exchange chamber (OPC-1; AutoMate Scientific) in which the bath could be changed in less than 1 s. The basic recording solution contained (in mM) 110 NaCl, 2 KCl, 3 $MgCl_2$, and 5 HEPES, pH 7.4. Ion substitutions are as described in Results.

Whole-cell currents were measured using a two-electrode voltage clamp (OC-725, Warner Instrument Corp.) with an ITC-16 interface (Instrutech/HEKA Instruments) running Pulse software (Heka Instruments). Pipette resistances were 0.5–1 MΩ when filled with 3 M KCl. For measurements of I-V relationships, the voltage was first clamped at the resting membrane potential and then changed to values between −150 and +100 mV in steps of 50-ms duration.

Patch clamp

Immediately before patch-clamp measurements, the vitelline membranes of the oocytes were mechanically removed in a hypertonic solution containing 200 mM sucrose. Patch-clamp pipettes were prepared from hematocrit capillary glass (VWR Scientific) using a three-stage vertical puller. They had resistances of 2–8 MΩ. The pipette solution contained (in mM) 110 NaCl or LiCl and 5 HEPES buffered to pH 7.4. Bath solutions contained (in mM) 110 NaCl, 2 KCl, 3 $MgCl_2$, and 5 HEPES buffered to pH 7.4 or 5.0. Measurements were made in cell-attached patches. Currents were recorded with an EPC-7 patch-clamp amplifier (Heka Instruments) and digitized with a Digidata 1332A interface (Axon Instruments). Data were filtered at 1 kHz and analyzed with pCLAMP9 software (Axon Instruments).

Data analysis

The voltage dependence of block of ENaC-mediated currents was assessed using the Woodhull equation (Woodhull, 1973),

$$I_{Na}(B) = I_{Na}(0)/(1 + [B]/K_I(V)), \quad (1)$$

where [B] is the concentration of the blocker B. The effect of voltage (V) on the inhibition constant K_I is given by

$$K_I(V) = K_I(0) \cdot \exp(F \cdot z \cdot \delta \cdot V/RT), \quad (2)$$

where δ is the electrical distance across the membrane, z is the valence of the blocker, and F, R, and T are constants.

```
                                    18'  21'
hASIC1a     479   GDIGGQMGLFIGASILTVLELFDYA   503
rαENaC      576   SNLGSQWSLWFGSSVLSVVEMAELI   600
rβENaC      518   SNLGGQFGFWMGGSVLCLIEFGEII   542
rγENaC      530   SNFGGQLGLWMSCSVVCVIEIIEVF   554
```

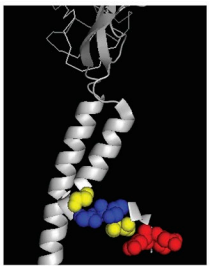

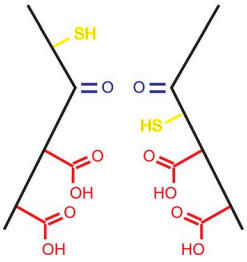

Figure 1. **Alignment of the C-terminal transmembrane domains of human ASIC1a and rat ENaC subunits.** The putative GAS selectivity region, named for the amino-acid sequence in ASIC1, is marked in blue, the conserved acidic amino acids in red, and the sites of Zn^{2+}-sensitive cysteine locations in yellow. Bottom: The transmembrane segments in one subunit of the putative open structure of chicken ASIC (Baconguis et al., 2014; PDB accession no. 4NTW), and a cartoon representation of the transmembrane pore. The relevant elements in TM2 are indicated with the same color scheme.

To analyze the effects of Na^+ on K^+ block, we assumed competitive inhibition such that

$$K_I(Na) = K_I(0)(1 + [Na^+]/K_{Na}) \quad (3)$$

where K_{Na} is the dissociation constant for Na^+ from the K^+ binding site.

Results

Fig. 1 aligns the sequences of the second transmembrane segments of rat ENaC and human ASIC1. In the region previously identified as the ENaC selectivity filter (Kellenberger et al., 1999a,b; Snyder et al., 1999; Sheng et al., 2000), the critical amino acid triplets are 587GSS in αENaC, 529GGS in βENaC, and 541SCS in γENaC. In hASIC1a, which forms a conducting homotrimer, the corresponding segment is 490GAS. Further downstream, two sets of acidic amino acids are conserved in ASIC1 and in all three ENaC subunits. These residues, designated as E18′ and E21′, are essential for the Na:K selectivity of ASIC1 (Lynagh et al., 2017).

Fig. 2 illustrates the Na:K selectivity of WT ENaC. α, β, and γENaC subunits were expressed in *Xenopus* oocytes and currents measured by two-electrode voltage clamp. Fig. 2 A illustrates typical current traces and I-V relationships in the WT channel. To assess currents through ENaC (I_{Na}), total current was corrected for that measured in the presence of 10 μM amiloride in the bath (Fig. 2 B). Fig. 2, C and D, shows I_{Na}-V relationships with either 110 mM NaCl or 110 mM KCl in the bath. With extracellular Na^+, currents were inward at membrane voltage (V_m) < 0 mV and reversed at V_m = 58 mV. When Na^+ was replaced by K^+, only outward amiloride-sensitive currents were observed, and no clear reversal potential could be identified. These data are consistent with a very high Na-to-K permeability ratio (P_{Na}/P_K) ratio and intracellular Na ∼11 mM, accounting for the outward currents.

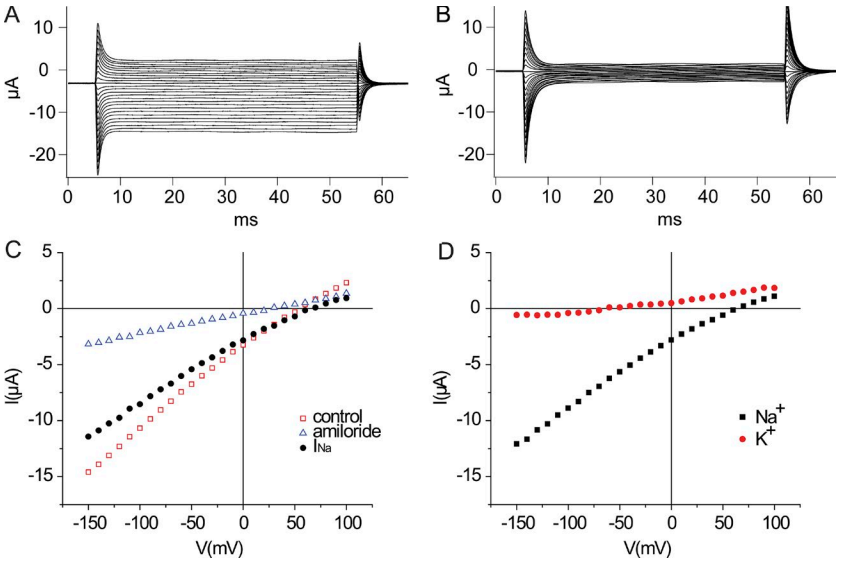

Figure 2. **Current-voltage relationships in ENaC-expressing oocytes. (A)** Currents in the presence of 110 mM extracellular Na^+. **(B)** Currents in the presence of 110 mM extracellular K^+. **(C)** I-V plots show currents as a function of voltage in the presence of Na^+ with and without 10 μM amiloride, and the difference currents (I_{Na}). **(D)** Amiloride-sensitive currents in the presence of Na^+ or K^+.

The permeability ratio could not be accurately determined, but assuming a reversal potential with K^+ of −100 mV, we estimate P_{Na}/P_K ~500, consistent with previous results in expression systems and native tissues (Garty and Palmer, 1997; Kellenberger and Schild, 2002).

Fig. 3 shows similar measurements obtained with the conserved E at position E18′ converted to Q in one of the subunits. In these oocytes, I_{Na} was smaller than for the WT channel, especially for the α E18′Q/β/γ construct (Table 1). Nevertheless, inward currents could be easily determined in the presence of Na^+, but not with K^+. For two of the mutants, α E18′Q/β/γ and α/β E18′Q/γ, the shape of the I_{Na}-V relationships was less linear than for WT. This property was not explored further. The main conclusion is that channels with one glutamate at any of the E18′ positions removed maintain a high Na:K selectivity.

Similar results were obtained for mutations at the E21′ position (Fig. 4). Again, currents with the substitution in just one of the subunits were substantially smaller than for WT, particularly for the α/βE2Q/γ construct (Table 1). Although there was a tendency for the reversal potential to shift to less positive values in the presence of Na^+, this finding is difficult to interpret without knowing the intracellular Na^+ concentration. As with E18′Q channels, inward currents could clearly be resolved with Na^+ but not with K^+ in the bathing medium. As best we can tell, mutation of one E21′ residue does not have a significant impact on the high Na:K selectivity of ENaC.

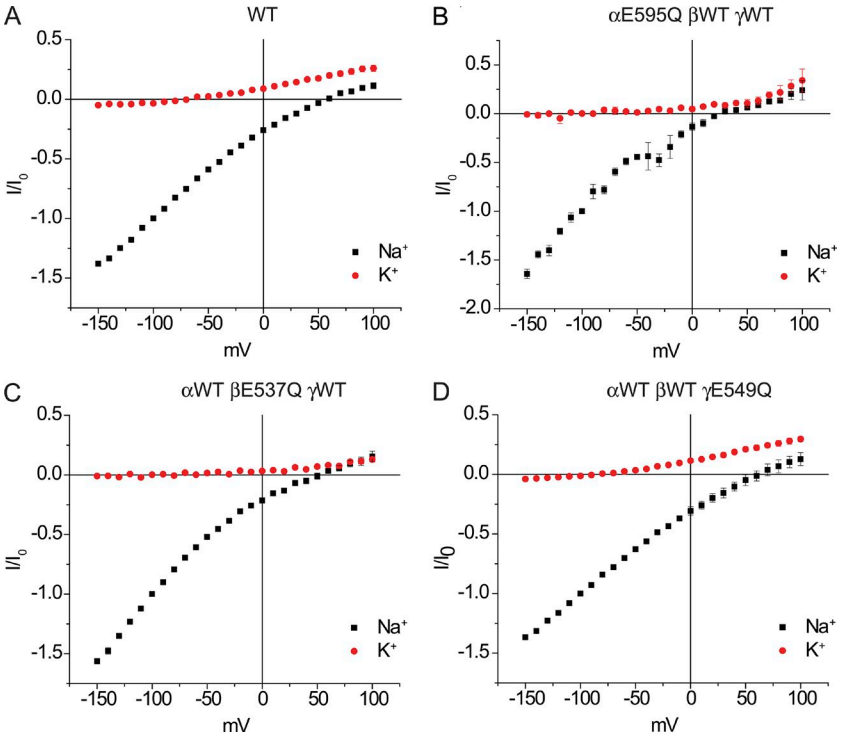

Figure 3. **Current-voltage relationships in the presence of 110 mM Na^+ and 110 mM K^+ in oocytes expressing ENaC with mutations in the E18′ positions. (A)** WT. **(B)** αE595Q/β/γ. **(C)** α/βE537Q/γ. **(D)** α/β/γE549Q. All data are corrected for amiloride-insensitive currents and normalized to the value at V_m = −100 mV in the presence of Na^+ (I_0). Data represent means ± SEM for four to seven oocytes.

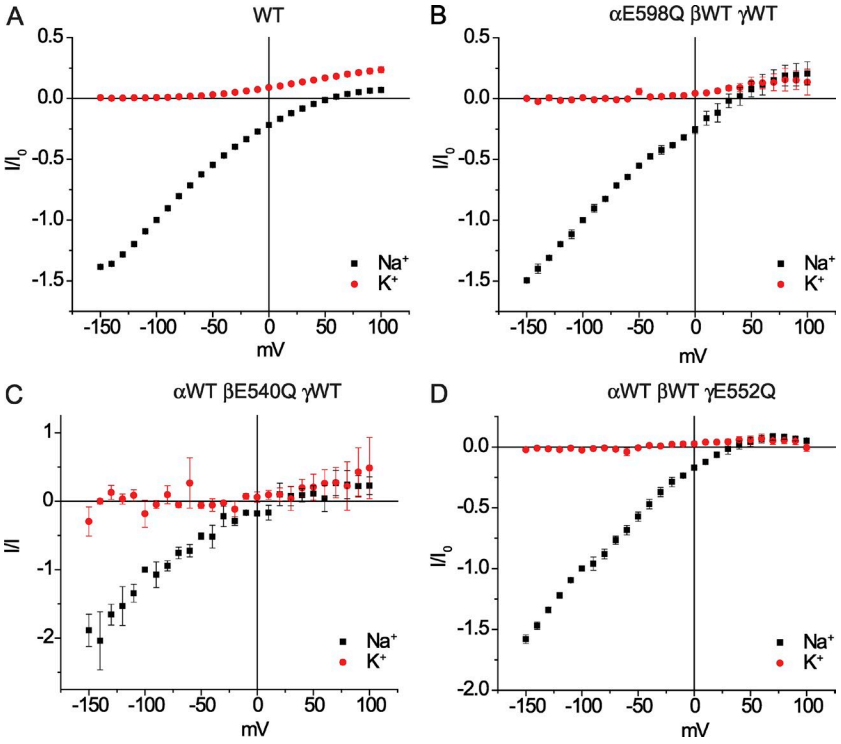

Figure 4. **Current-voltage relationships in the presence of 110 mM Na^+ and 110 mM K^+ in oocytes expressing ENaC with mutations in the E21′ positions. (A)** WT. **(B)** αE598Q/β/γ. **(C)** α/βE540Q/γ. **(D)** α/β/γE552Q. All data are corrected for amiloride-insensitive currents and normalized to the value at V_m = −100 mV in the presence of Na^+ (I_0). Data represent means ± SEM for three to seven oocytes.

Combining E-to-Q mutations in two of the subunits further decreased currents (Table 1), making selectivity measurements less reliable. We therefore attempted to increase ENaC function with gain-of-function mutations. Fig. 5 A shows that truncation of C-terminal tail of the βENaC subunit (β_T), mimicking a form of inherited hypertension called Liddle's syndrome (Schild et al., 1995), preserves high Na/K selectivity. Although the small inward currents in the presence of K^+ could represent conduction of that ion, we cannot rule out a contribution of Na^+ trapped in the extracellular space. This could occur during net efflux of Na^+ from the cell after removing the ion from the extracellular medium, particularly when the Na^+ permeability is high. Fig. 5 B illustrates results obtained with E18′Q mutants of α and γENaC expressed together with β_T. The small inward currents and large shift in reversal potential when Na^+ was replaced by K^+ indicate that selectivity was preserved in these channels. Fig. 5 C shows similar plots with E21′Q mutations in the α and γ subunits. The increased scatter in the plots reflects reduced signal-to-noise ratios. Here, both inward and outward currents were reduced with substitution of Na^+ by K^+. The reversal potential could not be reliably determined in the presence of K^+, but the lack of inward K^+ currents again implies that selectivity is maintained, at least as measured by conductance ratios.

We also used a second Liddle's syndrome mutation, α506S (Salih et al., 2017), to further augment channel activity. In Fig. 6 B we show that combining the α506S and β_T mutations maintains selectivity. Two double E18′Q mutants showed measurable current expression under these conditions, as illustrated in Fig. 6 C for α506S/β_TE18′Q/γE18′Q and in Fig. 6 D for α506SE18′Q/β_T/γE18′Q. Again, no inward currents were evident in the presence of K^+, implying preserved Na/K selectivity.

The difference between ASIC and ENaC with respect to E18′Q and E21′Q mutations might be due to the presence of a second rate-determining step in conduction through ENaC. This additional barrier could dominate the selectivity characteristics and

Table 1. **Amiloride-sensitive currents in oocytes expressing ENaC mutants**

Construct	I_{Na} (μA)	n
WT	12.1 ± 0.6	7
αE595Q/β/γ	1.2 ± 0.3	5
α/βE537Q/γ	6.1 ± 1.2	4
α/β/γE549Q	10.0±1.8	5
α/βE537Q/γE549Q	0.31 ± 0.06	4
αE595Q/β/γE549Q	0.22 ± 0.05	7
αE595Q/βE537Q/γ	0.13 ± 0.02	3
αE598Q/β/γ	2.5 ± 0.2	3
α/βE540Q /γ	0.43 ± 0.08	4
α/β/γE552Q	0.85 ±0.31	7
α/β_T/γ	11.3 ± 2.7	3
α5E95Q/β_T/γE549Q	0.22 ± 0.05	4
αE598Q/β_T/γE552Q	0.18 ± 0.06	5
WT	5.8 ± 0.5	3
αC506S/β/γ	13.6 ± 2.1	4
αC506S/β_T/γ	18.3 ± 1.4	5
αC506S,E595Q/β_T E573Q/γ	0.80 ± 0.16	3
αC506S/β_TE573Q/γE549Q	0.57 ± 0.09	4

Currents measured at V_m = −150 mV. Data given as means ± SEM.

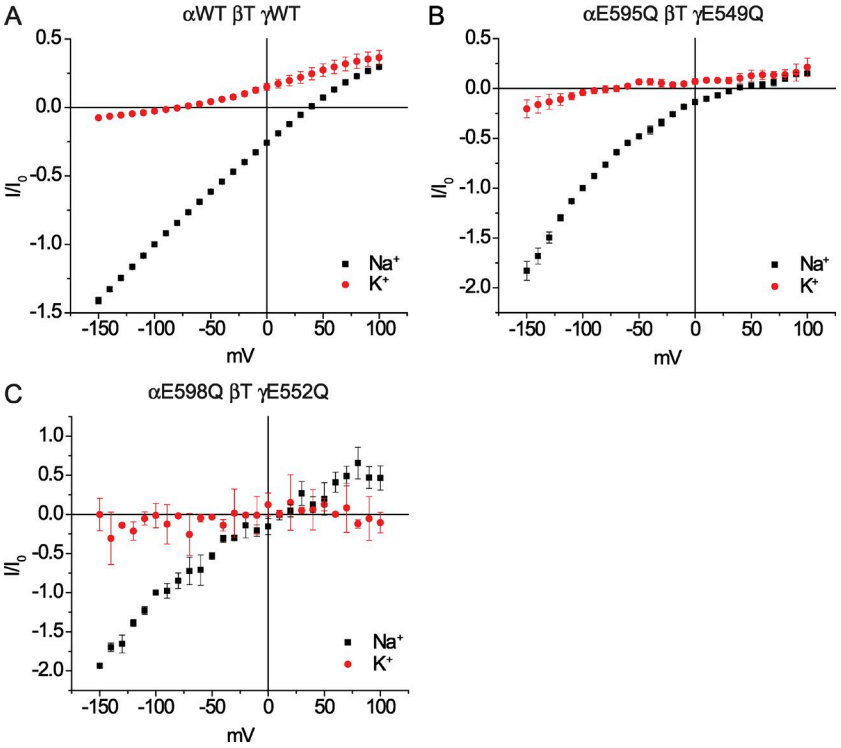

Figure 5. **Current-voltage relationships in the presence of 110 mM Na^+ and 110 mM K^+ in oocytes expressing ENaC with truncations in the β subunit. (A)** $\alpha/\beta_T/\gamma$. **(B)** αE595Q/β_T/γE549Q. **(C)** αE598Q/β_T/γE552Q. All data are corrected for amiloride-insensitive currents and normalized to the value at V_m = −100 mV in the presence of Na^+. Data represent means ± SEM for three to six oocytes.

confer the higher selectivity. Consistent with this notion, the single-channel conductance of ENaC is lower than that of ASIC under comparable conditions (Kellenberger and Schild, 2015). We therefore tested the possibility that E to Q mutations might change ENaC conductance without dramatically altering selectivity. Fig. 7 shows single-channel i-V relationships for WT as well as for the two E18′ mutants αE18′Q/β/γ and α/β/γE18′Q with Li^+ as the charge carrier. Although the i-V curves are shifted to some extent, probably reflecting differences in oocyte resting potential, the slopes are similar. If anything, the E18′Q mutants had slightly higher slope conductances for Li^+; in the case of α/β/γE18′Q, the change was statistically significant (P = 0.04). Lynagh et al. (2017) reported that substitution of D for E at the equivalent of the E18′ position decreased Na^+ conduction as well as Na/K

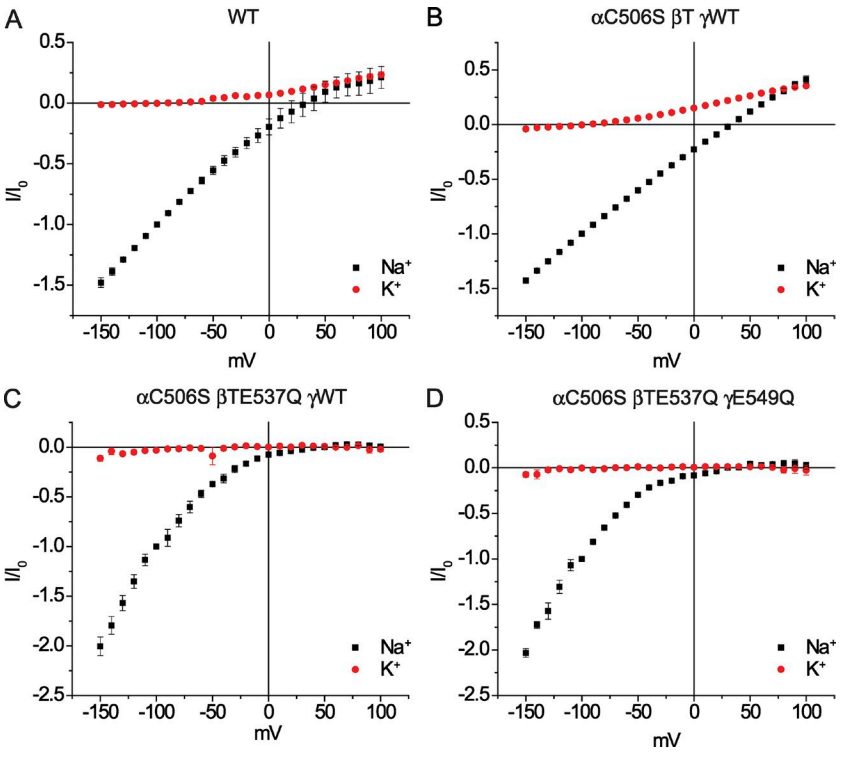

Figure 6. **Current-voltage relationships in the presence of 110 mM Na^+ and 110 mM K^+ in oocytes expressing ENaC with truncations in the β subunit and αC506S mutations. (A)** WT. **(B)** αC506S/β_T/γ. **(C)** αC506S E595Q/β_T/γ. **(D)** αC506S/β_TE537Q/γE549Q. All data are corrected for amiloride-insensitive currents and normalized to the value at V_m = −100 mV in the presence of Na^+. Data represent means ± SEM for three to six oocytes.

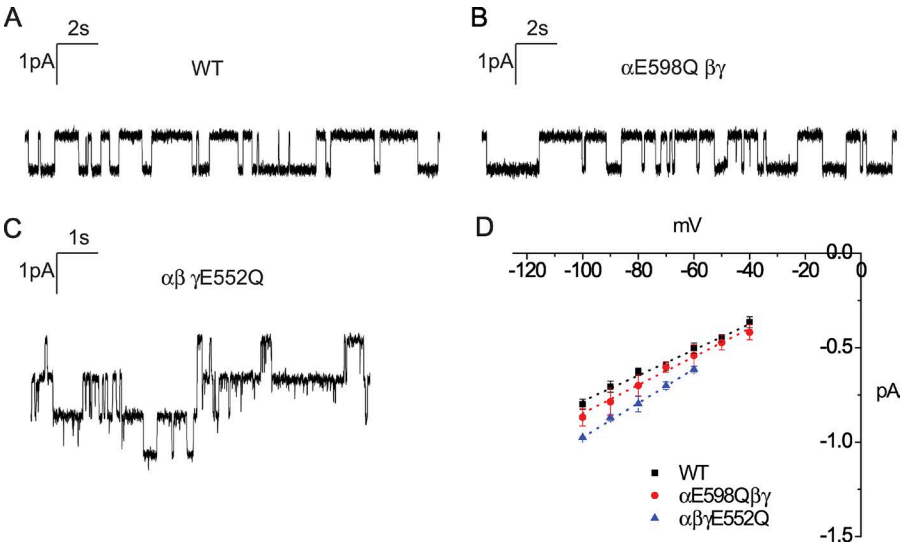

Figure 7. **Single-channel currents in E18′Q mutants.** Currents were recorded in the cell-attached mode at a pipette potential of +100 mV with 110 mM LiCl in the pipette. **(A)** WT ENaC. **(B)** αE598Q/β/γ. **(C)** α/β/γE552Q. **(D)** Single-channel i-V relationships for the channels shown in A through C. Data represent means ± SEM for two to seven patches. Slopes estimated by linear regression gave conductances of 6.9 ± 0.6 pS (WT), 7.6 ± 0.2 pS (αE598Q/β/γ), and 8.9 ± 0.2 pS α/β/γE552Q. The last value is significantly greater than that of the WT channel (P = 0.04).

selectivity. They also found that substitution of N for D at the equivalent of the E21′ position had no measurable effect on the single-channel conductance of ASIC1 to Na^+.

Limited magnitudes of expressed current weaken the conclusion that the selectivity filter for ENaC does not involve the E18′/E21′ locus. In particular, we could not measure any amiloride-sensitive current when either E18′ or E21′ residues were changed to Q in all three subunits. We therefore took an alternative approach to identifying the location of the filter. We reasoned that since K^+ cannot pass all the way through the channel, the extent to which it can penetrate the pore might be revealed from voltage-dependent block of Na^+ currents (Palmer, 1984).

We assessed the voltage dependence of block of WT ENaC by K^+ and guanidinium$^+$, two cations that do not permeate the entire channel. Fig. 8 A shows I_{Na}-V relationships with 20 mM Na^+ with and without 90 mM K^+. Consistent with previous results in native tissues (Palmer, 1984), K^+ blocked Na^+ currents. Woodhull analysis (Fig. 8 B) indicated a weak blocking affinity [Ki(0) = 450 mM] and a moderate voltage dependence (δ = 0.20). Adding guanidinium to the bath gave similar results (Fig. 9 A); Ki(0) for guanidinium was estimated to be 300 mM with δ = 0.24 (Fig. 9 B). Based on these results, we locate the site of block of ENaC by these two impermeant ions at ∼20% of the electric field.

To confirm that the K^+ blocking site is within the permeation pathway, we assessed whether its inhibition is competitive with Na^+, the natural "substrate" for the channel. We examined block by the same concentration of K^+ (70 mM) in the presence of either 10 mM or 40 mM Na^+ (Fig. 10, A and B). The apparent inhibition constant for K^+ at −100 mV was consistently higher at the larger Na^+ concentration (Fig. 10 C), as expected if block by K^+ required displacement of Na^+ from a site within the pore. Assuming a simple competitive interaction (see Materials and methods), we estimate an inhibition constant for K^+ of 126 ± 11 mM, and an affinity for Na^+ of 51 ± 10 mM at V_m = −100 mV. Both parameters decreased with more negative values of V_m (Fig. 10 D). The voltage dependence of K_{Na} diminishes at large negative potentials, perhaps because these voltages accelerate dissociation of Na^+ (but not K^+) ions from the binding site toward the cytoplasm. This is consistent with the idea that K^+ blocks Na^+ currents at a cation binding site within the pore that has a modest two- to threefold selectivity for Na^+:K^+.

The Woodhull analysis of voltage-dependent block (Woodhull, 1973) used in Figs. 8 and 9 indicates the site of block relative to the transmembrane electric field, rather than within the channel protein itself. To map the field onto the putative pore structure, we took advantage of earlier work using cysteine substitutions within the pore and divalent thiol-reactive cations such as Zn^{2+} and Cd^{2+} (Sheng et al., 2005; Takeda et al., 2007).

Adding a cys residue at αS583, extracellular to the GAS region (Fig. 1), conferred inhibition by extracellular Zn^{2+} (Takeda et al., 2007). The WT channel is slightly activated by Zn^{2+} (Fig. 11 A). Since Zn^{2+} block was rapid and easily reversible, we reasoned that it could be used to estimate the fraction of the electric field at the αS583 site. We confirmed Zn^{2+} block of the αS583C channel

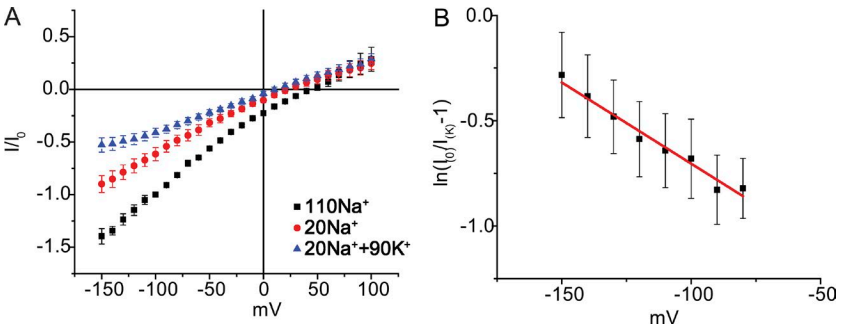

Figure 8. **Voltage dependence of block by K^+ in oocytes expressing ENaC. (A)** I_{Na}-V relationships in 20 mM NaCl with 90 mM $NMDG^+$ and no K^+, or 90 mM K^+. **(B)** Plot of $\ln(I_0/I_K - 1)$ versus voltage where I_0 and I_K are currents in the absence and presence of K^+, respectively. The slope of the relationship obtained by linear regression gives $K_K(0)$ = 450 ± 70 mM, $z \cdot \delta$ = 0.20 ± 0.03 (n = 5).

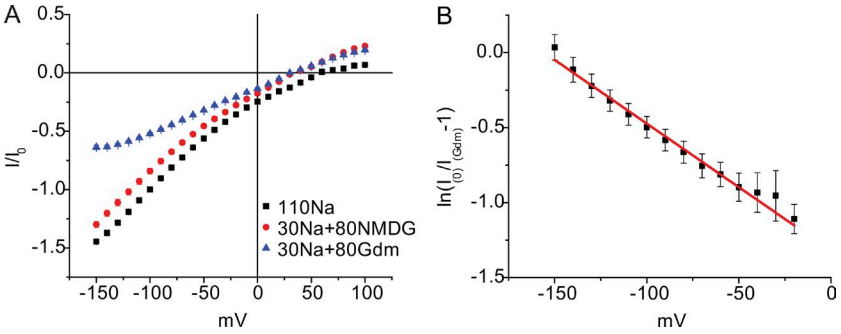

Figure 9. **Voltage dependence of block by guanidinium in oocytes expressing ENaC. (A)** I_{Na}-V relationships in 30 mM NaCl with 80 mM $NMDG^+$ and no guanidinium or 80 mM guanidinium. **(B)** Plot of $\ln(I_0/I_{gdm} - 1)$ versus voltage where I_0 and I_{gdm} are currents in the absence and presence of guanidinium, respectively. The slope of the relationship obtained by linear regression gives K_{gdm} (0) = 320 ± 40 mM, z•δ = 0.24 ± 0.02 (n = 6).

(Fig. 11 B). Furthermore, we found that the block was weakly voltage dependent; a Woodhull analysis yielded $K_I(0)$ = 270 µM and z • δ = 0.13 (Fig. 11 C), not taking into account possible stimulation by Zn^{2+}. If we assume that the mutant channels are activated, similar to WT through an independent effect of Zn^{2+}, the estimated z • δ decreases to 0.06 (Fig. 11 C). This is consistent with a location of αS583C ∼3–6% into the electric field from the outside.

This site is also thought to be close to the putative blocking site for amiloride (Schild et al., 1997; Sheng et al., 2000). We also examined the voltage dependence for amiloride block of the WT channel, estimating Ki(0) = 60 nM with δ = 0.03 (Fig. 12, A and B). For block of αS583C, for which amiloride affinity is reduced (Schild et al., 1997) we found $K_I(0)$ = 2 µM with δ = 0.12 (Fig. 12, C and D). All these data are consistent with an estimate of 3–12% of the electric field in a region just extracellular to the GAS region. Collectively, with the results of Fig. 11, these data indicate that K^+ can enter the pore from the outside beyond αS583, which is only one helical turn away from the GAS region.

Takeda et al. (2007) also showed that mutation of S589 in αENaC to C conferred sensitivity of currents to Zn^{2+} as well as Cd^{2+}. Since a similar block was found when S589 was changed to D, N, or A, it is presumably not a direct modification of the engineered cysteine side chain. However, as the effect was largely abolished by removal of a native cysteine (γC546S) deeper in the pore, they concluded that these mutations allowed divalent cations to penetrate the pore to reach γC546. They also assessed the voltage dependence of this interaction and estimated a δ value of 0.45. This suggests that the site of block by K^+ and guanidinium, and, by inference, the major selectivity filter in ENaC, is between the external Zn^{2+} (or amiloride) binding site and the conserved acidic region. This is consistent with the previous identification of the selectivity filter with the GAS region (Kellenberger and Schild, 2015).

We next asked if altering these amino acids to match those on the ASIC1 channel would recapitulate the ASIC1 selectivity pattern. To test this, we constructed three mutant ENaC subunits in which the putative selectivity regions αGSS, βGGS, and γSCS were all changed to GAS, the corresponding sequence in ASIC1 (Fig. 1). The corresponding channel, which we named $ENaC(GAS)_3$, expressed well, giving robust Na^+ currents. The Na^+/K^+ selectivity of the channel remained high, not detectably different from WT ENaC and much greater than the 8:1 selectivity of ASIC1 (Bässler et al., 2001; Li et al., 2011; Carattino and Della Vecchia, 2012; Yang and Palmer, 2014; Fig. 13). Furthermore, like WT ENaC and unlike ASIC1, $ENaC(GAS)_3$ did not conduct guanidinium to a measurable extent.

However, somewhat to our surprise, $ENaC(GAS)_3$ conducted Li^+ much better than Na^+ (Fig. 13). For the WT channel, inward

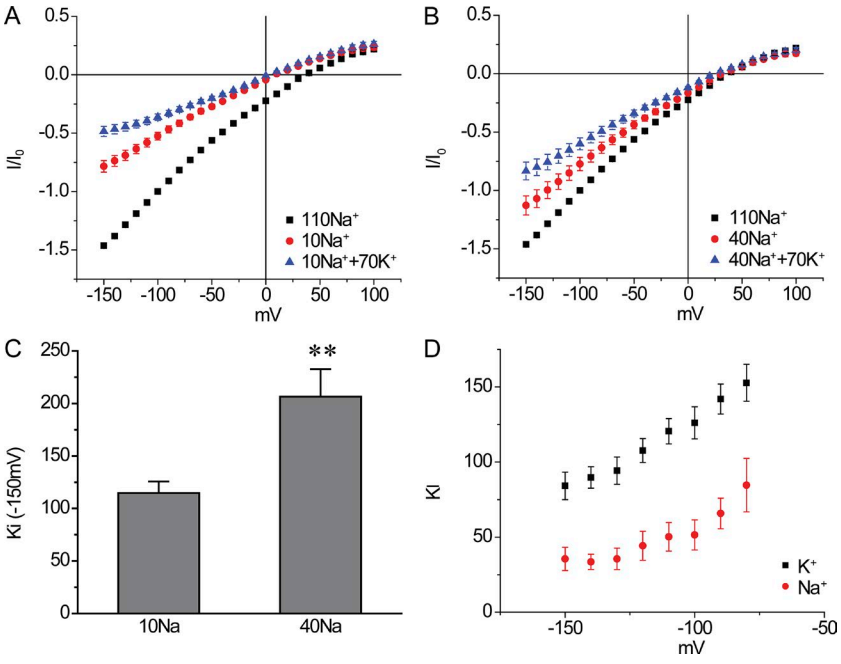

Figure 10. **Effect of Na^+ on block by K^+ in oocytes expressing ENaC. (A)** I_{Na}-V relationships in 10 mM Na^+ with and without 70 mM K^+. **(B)** I_{Na}-V relationships in 40 mM Na^+ with and without 70 mM K^+. **(C)** K_K at V_m = −150 mV with 10 and 40 mM Na^+. Values are significantly different (P = 0.002). **(D)** K_K and K_{Na} as a function of voltage.

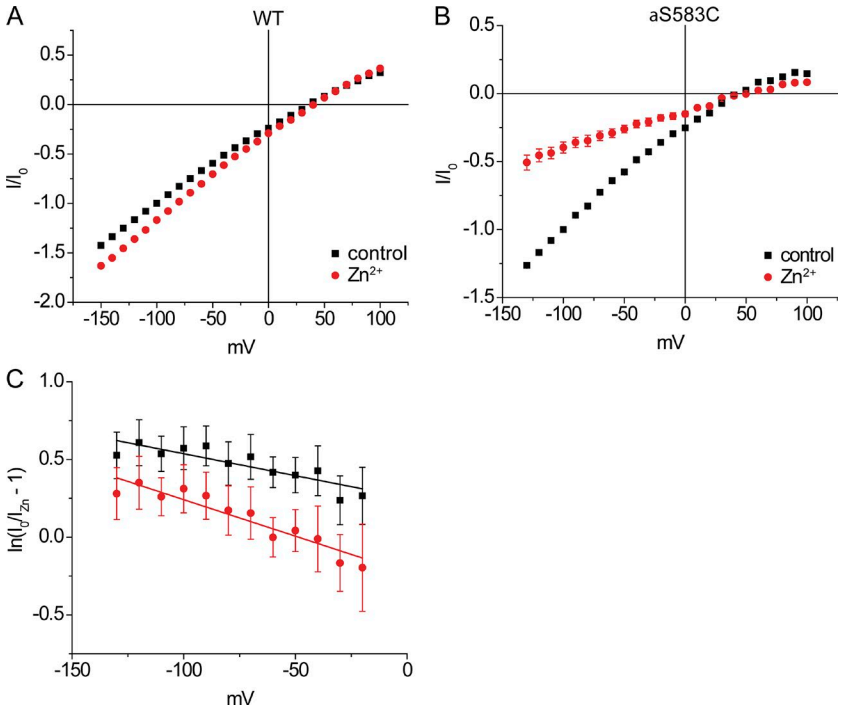

Figure 11. **Voltage dependence of block by Zn^{2+} in oocytes expressing αS583C/β/γ ENaC. (A)** I_{Na}-V relationships for WT ENaC in 110 mM NaCl with no Zn^{2+} and 0.2 mM Zn^{2+}. **(B)** I_{Na}-V relationships for ENaC αS583C/β/γ in 110 mM NaCl with no Zn^{2+} and 0.2 mM Zn^{2+}. **(C)** Plot of $\ln(I_0/I_{Zn} - 1)$ versus voltage, where I_0 and I_{Zn} are currents in the absence and presence of Zn^{2+}, respectively, for αS583C/β/γ. The slope of the relationship obtained by linear regression gives $K_{Zn}(0) = 230 \pm 40$ μM, $z\cdot\delta = 0.14 \pm 0.01$ ($n = 5$), assuming no stimulation of the channel by Zn^{2+} (red). Analysis assuming the same activation of WT and αS583C/β/γ gives $K_{Zn}(0) = 150 \pm 20$ μM, $z\cdot\delta = 0.06 \pm 0.01$ (black).

Li^+ currents were ~60% larger than Na^+ currents. With ENaC(-GAS)$_3$, the macroscopic current increased about threefold with Li^+ as the charge carrier. We made single-channel measurements to assess whether this difference reflected a higher conductance to Li^+ or a lower conductance to Na^+. As shown in Fig. 14, Li^+ currents were similar in the two channels, while Na^+ currents were substantially lower in the mutant. This high Li^+/Na^+ selectivity is not a property of ASIC1. Furthermore, the single-channel Na^+ conductance is larger in ASIC than in ENaC (Zhang and Canessa, 2002; Paukert et al., 2004; Yang and Palmer, 2014). Therefore, while subtle mutations in the GAS region can indeed alter permeation in ENaC, they do not account for the differences in the conductance properties of the two channels.

Discussion

Different selectivity properties of ENaC and ASIC

Although closely related in evolution, ENaC and ASIC have different selectivity properties (Kellenberger and Schild, 2002). While the permeability and conductance ratios for Na:K are ~8

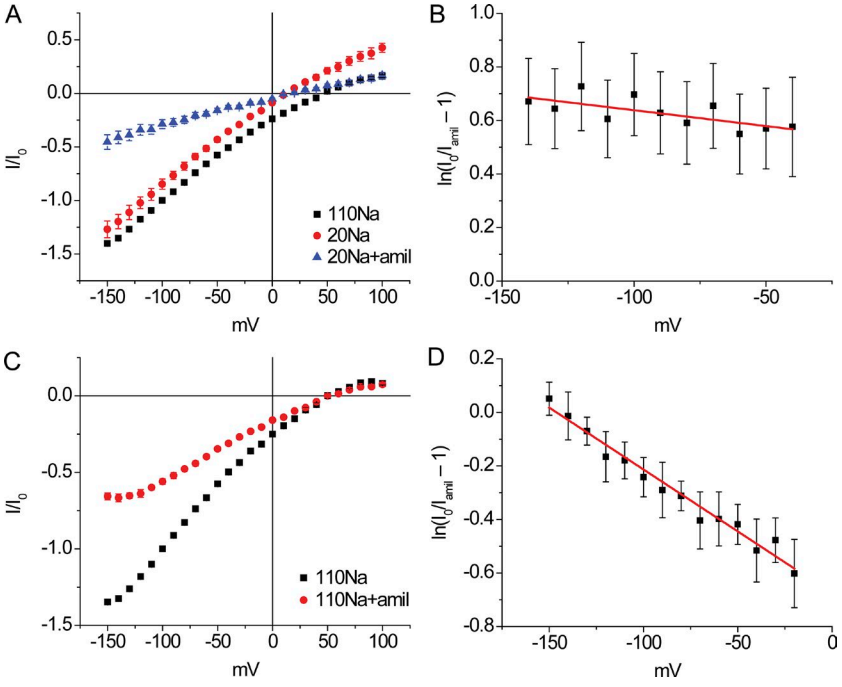

Figure 12. **Voltage dependence of block by amiloride in oocytes expressing WT and αS583C ENaC. (A)** I_{Na}-V relationships for WT in 20 mM NaCl with no amiloride or 0.1 μM amiloride (amil). **(B)** Plot of $\ln(I_0/I_{amil} - 1)$ versus voltage where I_0 and I_{amil} are currents in the absence and presence of amiloride, respectively. The slope of the relationship obtained by linear regression gives $K_{amil} = 64 \pm 11$ nM, $z\cdot\delta = 0.03 \pm 0.01$ ($n = 6$). **(C)** I_{Na}-V relationships for αS583C in 110 mM NaCl with no amiloride or 10^{-6} M amiloride. **(D)** Plot of $\ln(I_0/I_{amil} - 1)$ versus voltage. The slope of the relationship obtained by linear regression gives $K_{amil} = 2.0 \pm 0.2$ μM, $z\cdot\delta = 0.12 \pm 0.01$ ($n = 4$).

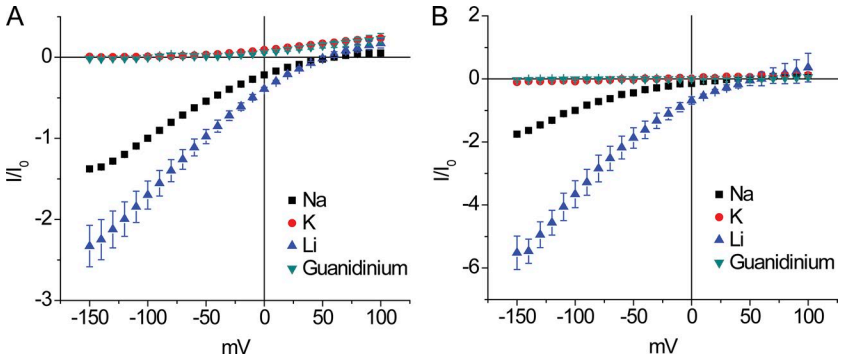

Figure 13. **Current-voltage relationships in WT ENaC and ENaC(GAS)$_3$. (A and B)** Currents were measured in the presence of 110 mM Na^+, 110 mM K^+, 110 mM guanidinium$^+$, and 110 mM Li^+ in oocytes expressing ENaC (A) and ENaC(GAS)$_3$ (B). All data are corrected for amiloride-insensitive currents and normalized to the value at V_m = −100 mV in the presence of Na^+. Data represent means ± SEM for three to eight oocytes.

in ASIC1 (Bässler et al., 2001; Li et al., 2011; Carattino and Della Vecchia, 2012; Yang and Palmer, 2014), the corresponding ratios are at least 10 times larger in ENaC (Palmer, 1982; Kellenberger et al., 1999b; Fig. 2), In addition, ASIC1 conducts small organic cations such as NH_4OH^+ and guanidinium$^+$ (Yang and Palmer, 2014), while ENaC does not (Palmer, 1982; Fig. 13). This very high selectivity makes sense in terms of the physiological roles of the two channels. Since ENaC transports Na^+ continuously, even a small leak of K^+ through the pore could impact the balance of this ion. ASIC, in contrast, is a sensory channel that opens transiently in response to an acid challenge and then quickly desensitizes. Any K^+ lost from the cell could be replenished from the extracellular fluid while the channels are closed.

Different sites for selectivity in ENaC and ASIC1

Our results together with those reported earlier for ENaC (Kellenberger et al., 1999a,b, 2001; Snyder et al., 1999; Sheng et al., 2000) and ASIC1 (Lynagh et al., 2017) suggest that the different selectivity properties of the two channels may reflect different selectivity filters rather than different properties of the same filter. Previous work using site-directed mutagenesis pointed to the GSS/GGS/SCS region of ENaC as a likely site of the selectivity filter. Even conservative mutations in these residues, without altering charge, in some cases had large impacts on the Na:K selectivity of the channels (Kellenberger et al., 1999a,b; Snyder et al., 1999; Sheng et al., 2000).

In ASIC, analysis of a putative open structure of the channel indicated that carbonyl oxygens of the GAS region formed the narrowest part of the transmembrane pore (Baconguis et al., 2014), consistent with a role of this region in determining conductance and selectivity. Indeed, decreasing the electric dipole of a backbone carbonyl in this region using unnatural amino acids increased Na:K selectivity, although Na^+ conductance was not affected (Lynagh et al., 2017).

In contrast, neutralizing conserved acidic residue in the more cytoplasmic aspect of the ASIC1 pore diminished its ability to discriminate between Na^+ and K^+; changing even a single E to Q at position E18′ significantly diminished both the Na:K and Na:Cs selectivities. Although ENaC also contains these negatively charged sites, our results indicate that while they are important for the formation and/or trafficking of functional channels, at least two of them can be deleted with preservation of high selectivity. This is consistent with a previous study of ENaC in which replacement of one of the conserved glutamates with arginine reduced macroscopic currents but not the high Na:K selectivity (Langloh et al., 2000). Of course, this does not

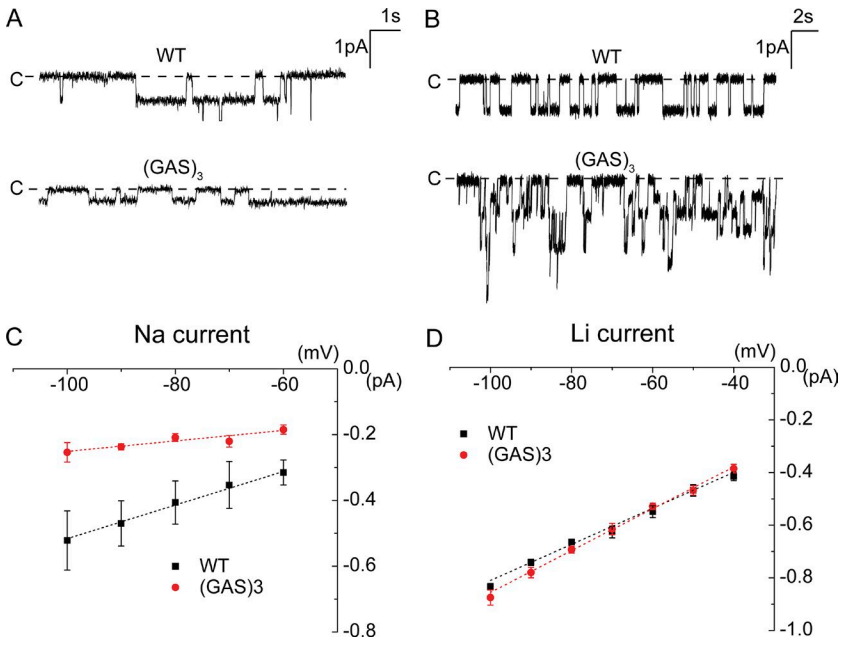

Figure 14. **Single-channel currents in WT ENaC and ENaC(GAS)$_3$.** Currents were recorded in the cell-attached mode at a pipette potential of +100 mV with 110 mM NaCl or 110 mM LiCl in the pipette. Top: Typical traces from WT and ENaC(GAS)$_3$. Bottom: i-V relationships. Data represent means ± SEM for three to five patches. Slope conductances for WT were 5.3 pS for Na^+ and 6.9 pS for Li^+. For ENaC(GAS)$_3$, they were 1.6 pS for Na^+ and 8.1 pS for Li^+.

preclude this or other parts of the channel from contributing to ion selectivity.

Mechanism of selectivity

Ion discrimination can result from selective ion binding to sites within the conduction pathway, or by selection according to size through molecular sieving. In the case of ASIC1, molecular dynamics simulations supported selective binding to the acidic regions implicated in the selectivity process (Lynagh et al., 2017). In contrast, there was no evidence for such a selective interaction with the GAS region. This is perhaps not surprising given the lack of negative charges to confer electrostatic interactions. In the case of ENaC, a selection by size seems more likely. Such a molecular sieve was proposed previously based on the finding that the only ions other than Na^+ that could readily permeate the channel are Li^+ and H^+, both of which have smaller atomic radii (Palmer, 1982). Kellenberger et al. (1999b) also analyzed site-directed mutagenesis data on the basis of changes in the size of the ENaC pore within the GSS/GGS/SCS region. With this interpretation, the altered selectivity of the ENaC $(GAS)_3$ mutant could arise from a slightly reduced pore radius, partially excluding Na^+ but not Li^+.

Pre-filter binding site

Our results do implicate selective binding at a site to the extracellular side of the selectivity filter; K^+ blocked Na^+ currents with low affinity in a voltage-dependent manner (Fig. 12). Competition experiments indicated an affinity of this site for Na^+ two to three times higher than that for K^+. The binding region has not been precisely identified, but based on the voltage dependence of block, it is likely to be between the Zn^{2+} interaction site at αS583C and the selectivity filter itself. Cation binding in this region may be stabilized by interactions with carbonyl oxygens lining the pore (Baconguis et al., 2014). This binding may contribute to, but clearly does not fully account for, the exquisite ability of ENaC to conduct Na^+ but not K^+.

Summary

While a recent study strongly implicates an acidic region of the transmembrane domain of ASIC1 in the process of selective ion permeation, our results do not support an important role of this part of ENaC in conferring the stronger selectivity characteristic of that channel. Our data are more consistent with the earlier identification of a selectivity filter closer to the amiloride-binding site near the outer aspect of the pore.

Acknowledgments

This work was supported by the National Institutes of Health (grant DK111380).

The authors declare no competing financial interests.

Author contributions: L. Yang carried out experiments and analyzed data. L.G. Palmer supervised the work and drafted the manuscript. Both authors designed experiments and edited the final manuscript.

Kenton J. Swartz served as editor.

Submitted: 21 June 2018
Accepted: 1 August 2018

References

Anantharam, A., Y. Tian, and L.G. Palmer. 2006. Open probability of the epithelial sodium channel is regulated by intracellular sodium. *J. Physiol.* 574:333–347. https://doi.org/10.1113/jphysiol.2006.109173

Baconguis, I., C.J. Bohlen, A. Goehring, D. Julius, and E. Gouaux. 2014. X-ray structure of acid-sensing ion channel 1-snake toxin complex reveals open state of a Na(+)-selective channel. *Cell.* 156:717–729. https://doi.org/10.1016/j.cell.2014.01.011

Bässler, E.L., T.J. Ngo-Anh, H.S. Geisler, J.P. Ruppersberg, and S. Gründer. 2001. Molecular and functional characterization of acid-sensing ion channel (ASIC) 1b. *J. Biol. Chem.* 276:33782–33787. https://doi.org/10.1074/jbc.M104030200

Canessa, C.M., L. Schild, G. Buell, B. Thorens, I. Gautschi, J.-D. Horisberger, and B.C. Rossier. 1994. Amiloride-sensitive epithelial Na^+ channel is made of three homologous subunits. *Nature.* 367:463–467. https://doi.org/10.1038/367463a0

Carattino, M.D., and M.C. Della Vecchia. 2012. Contribution of residues in second transmembrane domain of ASIC1a protein to ion selectivity. *J. Biol. Chem.* 287:12927–12934. https://doi.org/10.1074/jbc.M111.329284

Garty, H., and L.G. Palmer. 1997. Epithelial sodium channels: function, structure, and regulation. *Physiol. Rev.* 77:359–396. https://doi.org/10.1152/physrev.1997.77.2.359

Kellenberger, S., and L. Schild. 2002. Epithelial sodium channel/degenerin family of ion channels: a variety of functions for a shared structure. *Physiol. Rev.* 82:735–767. https://doi.org/10.1152/physrev.00007.2002

Kellenberger, S., and L. Schild. 2015. International Union of Basic and Clinical Pharmacology. XCI. structure, function, and pharmacology of acid-sensing ion channels and the epithelial Na+ channel. *Pharmacol. Rev.* 67:1–35. https://doi.org/10.1124/pr.114.009225

Kellenberger, S., I. Gautschi, and L. Schild. 1999a. A single point mutation in the pore region of the epithelial Na+ channel changes ion selectivity by modifying molecular sieving. *Proc. Natl. Acad. Sci. USA.* 96:4170–4175. https://doi.org/10.1073/pnas.96.7.4170

Kellenberger, S., N. Hoffmann-Pochon, I. Gautschi, E. Schneeberger, and L. Schild. 1999b. On the molecular basis of ion permeation in the epithelial Na+ channel. *J. Gen. Physiol.* 114:13–30. https://doi.org/10.1085/jgp.114.1.13

Kellenberger, S., M. Auberson, I. Gautschi, E. Schneeberger, and L. Schild. 2001. Permeability properties of ENaC selectivity filter mutants. *J. Gen. Physiol.* 118:679–692. https://doi.org/10.1085/jgp.118.6.679

Langloh, A.L., B. Berdiev, H.L. Ji, K. Keyser, B.A. Stanton, and D.J. Benos. 2000. Charged residues in the M2 region of alpha-hENaC play a role in channel conductance. *Am. J. Physiol. Cell Physiol.* 278:C277–C291. https://doi.org/10.1152/ajpcell.2000.278.2.C277

Li, T., Y. Yang, and C.M. Canessa. 2011. Asp433 in the closing gate of ASIC1 determines stability of the open state without changing properties of the selectivity filter or Ca2+ block. *J. Gen. Physiol.* 137:289–297. https://doi.org/10.1085/jgp.201010576

Lynagh, T., E. Flood, C. Boiteux, M. Wulf, V.V. Komnatnyy, J.M. Colding, T.W. Allen, and S.A. Pless. 2017. A selectivity filter at the intracellular end of the acid-sensing ion channel pore. *eLife.* 6:e24630. https://doi.org/10.7554/eLife.24630

Palmer, L.G. 1982. Ion selectivity of the apical membrane Na channel in the toad urinary bladder. *J. Membr. Biol.* 67:91–98. https://doi.org/10.1007/BF01868651

Palmer, L.G. 1984. Voltage-dependent block by amiloride and other monovalent cations of apical Na channels in the toad urinary bladder. *J. Membr. Biol.* 80:153–165. https://doi.org/10.1007/BF01868771

Palmer, L.G. 1987. Ion selectivity of epithelial Na channels. *J. Membr. Biol.* 96:97–106. https://doi.org/10.1007/BF01869236

Paukert, M., E. Babini, M. Pusch, and S. Gründer. 2004. Identification of the Ca2+ blocking site of acid-sensing ion channel (ASIC) 1: implications for channel gating. *J. Gen. Physiol.* 124:383–394. https://doi.org/10.1085/jgp.200308973

Salih, M., I. Gautschi, M.X. van Bemmelen, M. Di Benedetto, A.S. Brooks, D. Lugtenberg, L. Schild, and E.J. Hoorn. 2017. A Missense Mutation in the Extracellular Domain of αENaC Causes Liddle Syndrome. *J. Am. Soc. Nephrol.* 28:3291–3299. https://doi.org/10.1681/ASN.2016111163

Schild, L., C.M. Canessa, R.A. Shimkets, I. Gautschi, R.P. Lifton, and B.C. Rossier. 1995. A mutation in the epithelial sodium channel causing Liddle disease increases channel activity in the Xenopus laevis oocyte expression system. *Proc. Natl. Acad. Sci. USA.* 92:5699–5703. https://doi.org/10.1073/pnas.92.12.5699

Schild, L., E. Schneeberger, I. Gautschi, and D. Firsov. 1997. Identification of amino acid residues in the alpha, beta, and gamma subunits of the epi-

thelial sodium channel (ENaC) involved in amiloride block and ion permeation. *J. Gen. Physiol.* 109:15–26. https://doi.org/10.1085/jgp.109.1.15
Sheng, S., J. Li, K.A. McNulty, D. Avery, and T.R. Kleyman. 2000. Characterization of the selectivity filter of the epithelial sodium channel. *J. Biol. Chem.* 275:8572–8581. https://doi.org/10.1074/jbc.275.12.8572
Sheng, S., C.J. Perry, O.B. Kashlan, and T.R. Kleyman. 2005. Side chain orientation of residues lining the selectivity filter of epithelial Na+ channels. *J. Biol. Chem.* 280:8513–8522. https://doi.org/10.1074/jbc.M413880200
Snyder, P.M., D.R. Olson, and D.B. Bucher. 1999. A pore segment in DEG/ENaC Na(+) channels. *J. Biol. Chem.* 274:28484–28490. https://doi.org/10.1074/jbc.274.40.28484
Takeda, A.N., I. Gautschi, M.X. van Bemmelen, and L. Schild. 2007. Cadmium trapping in an epithelial sodium channel pore mutant. *J. Biol. Chem.* 282:31928–31936. https://doi.org/10.1074/jbc.M700733200
Woodhull, A.M. 1973. Ionic blockage of sodium channels in nerve. *J. Gen. Physiol.* 61:687–708. https://doi.org/10.1085/jgp.61.6.687
Yang, L., and L.G. Palmer. 2014. Ion conduction and selectivity in acid-sensing ion channel 1. *J. Gen. Physiol.* 144:245–255. https://doi.org/10.1085/jgp.201411220
Zhang, P., and C.M. Canessa. 2002. Single channel properties of rat acid-sensitive ion channel-1alpha, -2a, and -3 expressed in Xenopus oocytes. *J. Gen. Physiol.* 120:553–566. https://doi.org/10.1085/jgp.20028574